ECCOMAS Congress 2016
VII European Congress on Computational Methods in Applied Sciences and Engineering
M. Papadrakakis, V. Papadopoulos, G. Stefanou, V. Plevris (eds.)
Crete Island, Greece, 5–10 June 2016

A CONSISTENTLY LINEARISED SOLID MECHANICS-BASED MESH DEFORMATION TECHNIQUE FOR HIGH ORDER CURVED ELEMENTS

Roman Poya[1], **Ruben Sevilla**[1], **and Antonio J. Gil**[1]

[1]Zienkiewicz Centre for Computational Engineering, College of Engineering, Swansea University Bay Campus, Crymlyn Burrows, Swansea SA1 8EN, UK

e-mail: {R.Poya, R.Sevilla, A.J.Gil}@swansea.ac.uk

Keywords: Mesh deformation, curved elements, high order methods, distortion measure, solid mechanics analogy.

Abstract. *In this work, a novel solid mechanics-based mesh deformation technique for high order curved elements is presented. The technique falls under the a posteriori curved mesh generation category, where higher order nodes are placed on a linear mesh and the geometry is then deformed to conform to the exact CAD boundary. In contrast to the existing a posteriori approaches in the literature such as the techniques based on the inclusion of residual stresses, parametrised and varying material constants, regularisation and smoothing of curved meshes, in this work, a rather consistent solid mechanics approach is followed. This implies, that the underlying Euler-Lagrange equations that need to be solved for, emerge from an energy principle, with well-defined internal energies constructed for an hyperelastic system, which are subsequently, consistently linearised. Depending on the geometrical parameterisation, the approach guarantees better mesh quality and lower condition number for the system of equations. Furthermore, due to the introduction of independent invariants emanating from fibre, surface and volume mappings, the essential mesh distortion measures are encoded in the formulation. The paper proves that for for two-dimensional elements such as triangles and quadrilaterals, not all the distortion measures can be independent. An example of materially instable internal energy is provided to pinpoint the importance of a consistent formulation in the context of highly stretched boundary layer meshes.*

1 INTRODUCTION

The use of curved elements is nowadays accepted to be crucial in order to fully exploit the advantages of high-order discretisation methods, but until relatively recently, the challenge of automatically generating high-order curvilinear meshes has been an obstacle for the widespread application of high-order methods [Vincent and Jameson(2011)]. Methods to produce high-order curvilinear meshes are traditionally classified into *direct* methods and *a posteriori* methods [Dey, O'Bara, and Shephard]. Direct methods build the curvilinear high-order mesh directly from the CAD boundary representation of the domain whereas a posteriori approaches rely on mature low-order mesh generation algorithms to produce an initial mesh that is subsequently curved using different techniques, such as local modification of geometric entities, solid mechanics analogies or optimisation.

Within the category of a posteriori approaches, the solid mechanics analogy first proposed in [Persson and Peraire] has become increasingly popular. The main idea is to consider the initial, low-order, mesh as the undeformed configuration of an elastic solid. High-order nodal distributions are then inserted into all of the elements and then the nodes over element edges/faces in contact with the curved parts of the boundary are projected onto the true CAD boundary. The displacement required to move the nodes onto the true boundary is interpreted as an essential boundary condition within the solid mechanics analogy. The solution of the elastic problem provides the desired curvilinear mesh as the deformed configuration. The initial approach proposed in [Persson and Peraire] used a non-linear neo-Hookean constitutive model. Several attempts to reduce the computational cost of this approach have been proposed based on a linear elastic analogy, see [Xie, Sevilla, Hassan, and Morgan]. It is clear that when large deformations are induced to produce the deformed curvilinear high-order mesh, a linear elastic model can result in non-valid elements due to the violation of the hypothesis of small deformations. In order to alleviate this problem, it is possible to split the desired (potentially large) displacement of boundary nodes into smaller load increments. Other approaches to increase the robustness of the linear elastic analogy have been recently introduced, see for instance [Moxey, Ekelschot, Keskin, Sherwin, and Peiró], where *pseudo* thermal effects are introduced.

In this work, a novel a posteriori solid mechanics-based mesh deformation technique for high order curved elements is presented. In contrast to the existing a posteriori approaches in the literature such as the techniques based on the inclusion of residual stresses, parametrised and varying material constants, regularisation and smoothing of curved meshes, in this work, a rather consistent solid mechanics approach is followed. This implies, that the underlying Euler-Lagrange equations that need to be solved for, emerge from an energy principle, with well-defined internal energies constructed for an hyperelastic system, which are subsequently, consistently linearised. The theoretical and computational framework is presented in the next two sections, respectively and finally followed by the numerical examples sections.

2 NO-LINEAR CONTINUUM MECHANICS

Let us consider the motion of a continuum from its initial undeformed (or material) configuration $\Omega_0 \subset \mathbb{R}^d$, with boundary $\partial\Omega_0$ and outward unit normal $\boldsymbol{n}_0$, into its final deformed (or spatial) configuration $\Omega \subset \mathbb{R}^d$, with boundary $\partial\Omega$ and outward unit normal $\boldsymbol{n}$, where d represents the number of spatial dimensions. In the context of curved mesh generation, the initial (undeformed) configuration Ω_0 represents a linear mesh with planar faces (edges in two dimensions) and the final (deformed) configuration Ω represents the final curved high-order mesh, as illustrated in Figure 1. The motion is described by a mapping $\boldsymbol{\phi}$ which links a material particle

from material configuration $\boldsymbol{X}$ to spatial configuration $\boldsymbol{x}$ according to $\boldsymbol{x} = \boldsymbol{\phi}(\boldsymbol{X})$.

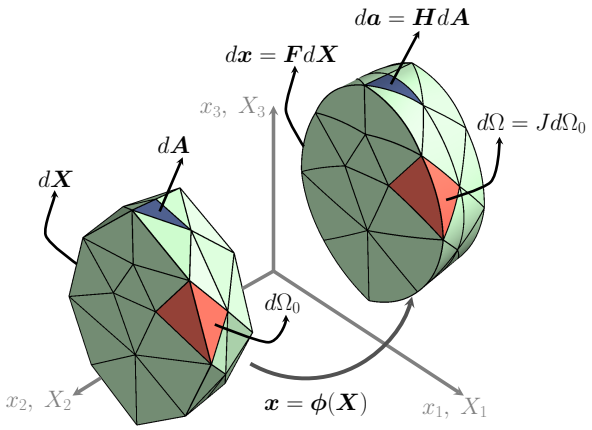

Figure 1: Deformation map of a continuum and illustration of the strain measures $\boldsymbol{F}$, $\boldsymbol{H}$ and J.

The following well-known strain measures can be introduced, namely the two-point deformation gradient tensor or fibre-map $\boldsymbol{F}$, the two-point co-factor or adjoint tensor or area map $\boldsymbol{H}$ and the Jacobian J or volume-map

$$\boldsymbol{F} = \boldsymbol{\nabla}_0 \boldsymbol{\phi} = \frac{\partial \boldsymbol{\phi}}{\partial \boldsymbol{X}}, \qquad \boldsymbol{H} = J \boldsymbol{F}^{-T}, \qquad J = \frac{1}{3} \boldsymbol{H} : \boldsymbol{F} \tag{1}$$

where $\boldsymbol{\nabla}_0$ denotes the gradient with respect to material coordinates. The fundamental strain measures $\{\boldsymbol{F}, \boldsymbol{H}, J\}$, also illustrated in Figure 1, encode the essential modes of deformation, based on which a complete set of indepdendent mesh quality/distortion measure can be defined. Kinematically any other quality measure would be a combination of these three measures.

3 A CONSISTENT INCREMENTALLY LINEARISED APPROACH

To guarantee and/or maintain essential mathematical requirements such as objectivity and polyconvexity for the linearised strain energy density, a linearised solid mechanics approach must emanate from an underlying non-linear variational principle, as the notion of objectivity and polyconvexity cannot be invoked in small strains. This is typically achieved by consistent linearisation of the non-linear total potential energy through a Taylor series expansion. To illustrate this, let us consider the total potential energy in non-linear system, cast in the form of an iterative (Newton-Raphson) scheme

$$\Pi(\boldsymbol{\phi}^{\star}_{n+1}) = \inf_{\boldsymbol{\phi}_{n+1} \in \boldsymbol{\mathcal{V}}_{n+1}} \left\{ \int_{\Omega_0} \Psi(\boldsymbol{C}_{n+1})\, d\Omega_0 \right\} \tag{2}$$

where $\boldsymbol{\mathcal{V}}_{n+1} = \left\{ \boldsymbol{\phi}_{n+1} \in [\mathcal{H}^1(\Omega_0)]^d \ : \ \boldsymbol{\phi}_{n+1}(\boldsymbol{X}) = \bar{\boldsymbol{x}}_{n+1} \text{ on } \partial\Omega_0 \right\}$ and $\boldsymbol{x}_{n+1} = \boldsymbol{\phi}_{n+1}(\boldsymbol{X})$ is the position vector of the material points at increment $n+1$, which can be evaluated through an incremental displacement $\boldsymbol{u}$ superimposed on the deformed configuration at increment n, i.e. $\boldsymbol{x}_{n+1} = \boldsymbol{x}_n + \boldsymbol{u}$. At increment n, the current position vector $\boldsymbol{x}_n$, the state of deformation gradient $\boldsymbol{F}_n$ and, subsequently, the Cauchy-Green strain $\boldsymbol{C}_n$ are fully known. In a non-linear regime, the motion of the continuum from n to $n+1$ is solved iteratively, as the amount of displacements,

the state of deformation gradient $\boldsymbol{F}_{n+1}$ and the Cauchy-Green strain $\boldsymbol{C}_{n+1}$ cannot be determined explicitly.

However, in the context of high-order curved mesh generation, it is convenient to approximate (2) through a Taylor series expansion of the form

$$\Pi_u(\boldsymbol{u}^\star) = \inf_{\boldsymbol{u}\in\boldsymbol{\mathcal{U}}} \left\{ \int_{\Omega_0} \left(D\Psi(\boldsymbol{C}_n)[\boldsymbol{u}] + \frac{1}{2} D^2\Psi(\boldsymbol{C}_n)[\boldsymbol{u};\boldsymbol{u}] \right) d\Omega_0 \right\}. \tag{3}$$

where $\boldsymbol{\mathcal{U}} = \left\{ \boldsymbol{u} \in [\mathcal{H}^1(\Omega_n)]^d \ : \ \boldsymbol{u} = \bar{\boldsymbol{u}} \text{ on } \partial\Omega_n \right\}$. Notice that the first term in Taylor series expansion i.e. $\Psi(\boldsymbol{C})$ would be a constant term describing the state of strain energy density at increment n, which vanishes at the moment of computing the stationary point of (3). Certainly, embedded in the definition of the new total potential energy (Π_{lin}) in (3) are the first and second directional derivatives of the non-linear total potential energy. The spatial form of the linearised total potential energy can now be obtained as

$$\Pi_u(\boldsymbol{u}^\star) = \inf_{\boldsymbol{u}\in\boldsymbol{\mathcal{U}}} \left\{ \int_{\Omega_n} \left(\boldsymbol{\sigma}_n : \boldsymbol{\varepsilon}_n(\boldsymbol{u}) + \frac{1}{2}\, \boldsymbol{\varepsilon}_n(\boldsymbol{u}) : \boldsymbol{c}_n : \boldsymbol{\varepsilon}_n(\boldsymbol{u}) + \frac{1}{2}\, \boldsymbol{\sigma}_n : \left((\nabla_n \boldsymbol{u})^T (\nabla_n \boldsymbol{u}) \right) \right) d\Omega_n \right\} \tag{4}$$

where the subscript n denotes the state of deformation, stresses, tangent elasticity and the volume at increment n, namely $\boldsymbol{\varepsilon}_n$, $\boldsymbol{\sigma}_n$, $\boldsymbol{c}_n$ and Ω_n. In addition, ∇_n represents the spatial gradient operator at increment n. The stationary condition of (4), obtained after the linearisation with respect to the virtual displacement $\boldsymbol{v}$, leads to the principle of virtual work

$$D\Pi_u(\boldsymbol{u}^\star)[\boldsymbol{v}] = \int_{\Omega_n} \left(\underbrace{\boldsymbol{\sigma}_n : \boldsymbol{\varepsilon}_n(\boldsymbol{v})}_{\mathcal{R}_n} + \underbrace{\boldsymbol{\varepsilon}_n(\boldsymbol{u}) : \boldsymbol{c}_n : \boldsymbol{\varepsilon}_n(\boldsymbol{v})}_{\mathcal{C}_n} + \underbrace{\boldsymbol{\sigma}_n : ((\nabla_n \boldsymbol{u})^T (\nabla_n \boldsymbol{v}))}_{\mathcal{G}_n} \right) d\Omega_n = 0. \tag{5}$$

It is worth noting that, in the right hand side of (5), the first term $\mathcal{R}_n$ corresponds to the residual stresses, the second term $\mathcal{C}_n$ to the linearised constitutive stiffness term and the last term $\mathcal{G}_n$ to the geometric stiffness term. The emergence of the geometric stiffness term is due to consistent linearisation of the non-linear total potential energy, which would not have appeared, had the starting point not been chosen to correspond to a non-linear total potential energy. As will be seen in the numerical examples, in the context of high-order curved mesh generation, the geometric stiffness term, stiffens the interior elements of the computational mesh against severe distortion, hence producing meshes with better quality. Note that unlike in the non-linear analysis, since (5) is linear in $\boldsymbol{u}$, a further linearisation is not required. It is evident that, if a single increment is used to reach the final configuration, i.e. when $n = 0$, the equations of classical linear elasticity are recovered.

4 QUALITY MEASURES

In a standard high-order finite element formulation, measures involving the Jacobian of the isoparametric mapping have been extensively used, in particular the so-called scaled Jacobian. This measure only quantifies volumetric deformations and alternative measures that exploit different modes of deformation and account for shape, skewness and degeneracy of elements can also be considered. However, it is worth noting that not all of these quality measures can be regarded as independent quantities. From a solid mechanics point of view, only three independent isotropic and two independent transversely isotropic quality measures for a generic

element e can be introduced

$$Q_j^e = \sqrt{\frac{\min_{\boldsymbol{\xi} \in R} \{I_j\}}{\max_{\boldsymbol{\xi} \in R} \{I_j\}}} \qquad \text{for } j = 1, \ldots, 5, \tag{6}$$

where R denotes the reference element employed in the isoparametric formulation, with local coordinates $\boldsymbol{\xi}$. If necessary, further quality measures can be obtained through a linear combination of the invariants I_j which will be independent of the geometrical parametrisation.

5 NUMERICAL EXAMPLES

This section presents a few selected numerical examples. For all the examples, material parameters are chosen as $E = 10^5$ for Young's modulus, $E_A = \frac{5E}{2}$ for transversely isotropic bending modulus and $G_A = \frac{E}{2}$ for transversely isotropic shear modulus and the Poisson's ratio is varied within the interval [0.001,0.495].

The first example considers an anisotropic boundary layer mesh around the SD7003 aerofoil with a stretching level of 25 in the boundary layer. The detailed view near the leading edge of the initial linear triangular and the high order mesh with a degree approximation of $p = 5$ is shown in Figure 2 having 27,410 nodes. The curvilinear mesh is obtained using 20 load increments of a consistently linearised version of Neo-Hookean model. The minimum quality measures characterising fibre, surface and volume deformation are, $Q_1 = 0.991$, $Q_2 = 0.991$ and $Q_3 = 0.982$, respectively, numerically confirming that the first two quality measures (related to fibre and surface deformation) are identical in two-dimension.

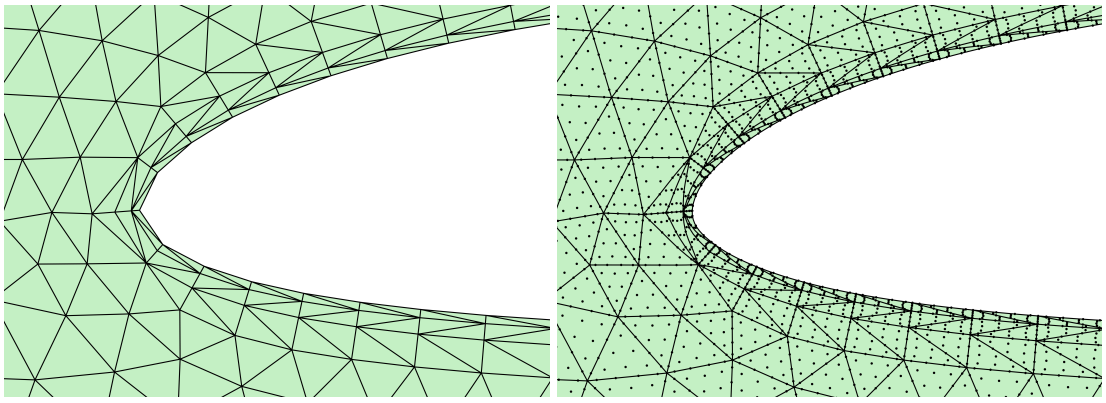

(a) Linear mesh. (b) High-order mesh with p=5.

Figure 2: Boundary layer mesh around an aerofoil.

The next example considers an isotropic tetrahedral mesh around a cylinder. The initial linear and the high order mesh with a degree approximation of $p = 4$ is shown in Figure 3 having 38,355 nodes. The curvilinear mesh is obtained using 30 load increments of a consistently linearised version of nearly incompressible Mooney-Rivlin type material model. The minimum quality measures characterising fibre, surface and volume deformation are, $Q_1 = 0.965$, $Q_2 = 0.928$ and $Q_3 = 0.891$, respectively. Note that nodes lying on the planar faces of cylinder require in-plane translation.

Finally 5 pin-points two critical aspects of solid mechanics based curved mesh generation approaches, namely, the importance of a well-defined (i.e. polyconvex) material model depicted in 5a (note that all material models apart form ILE TI and CIL TI models are well defined;

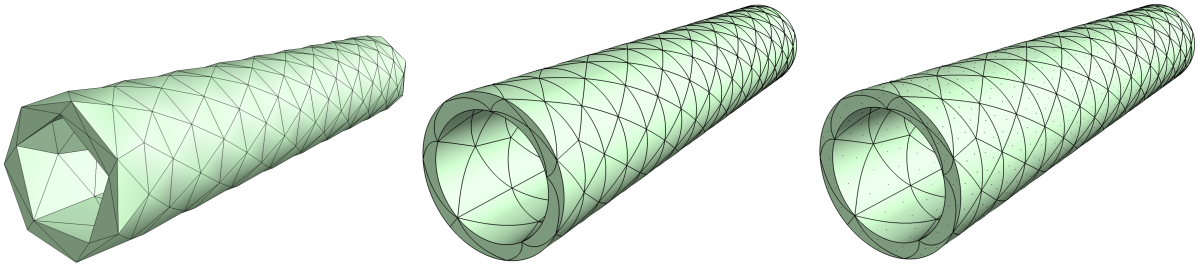

(a) Linear surface mesh. (b) $p = 4$ surface mesh (c) $p = 4$ mesh surface showing nodes

Figure 3: Isotropic mesh around cylinder.

notice the drop in mesh quality associated with these material models), and the equivalence of fibre quality and surface quality i.e. $Q_1 = Q_2$ for two-dimensional problems shown in 5b; both for anisotropic boundary layer mesh. For the explicit forms of the material models refer to [Poya, Sevilla, and Gil].

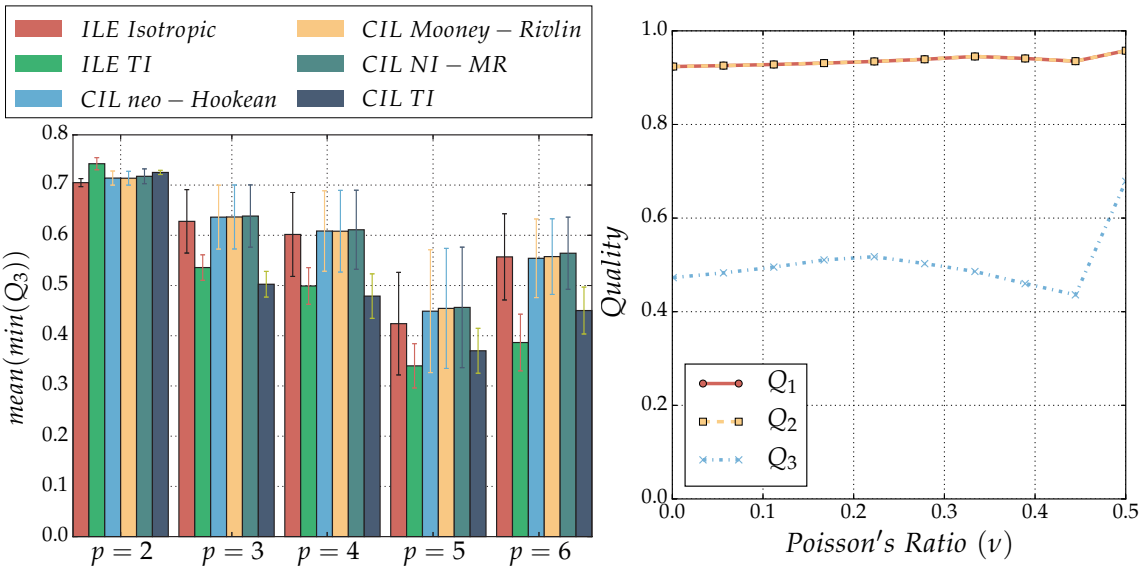

(a) Mean value and standard deviation of the minimum scaled Jacobian of the generated meshes as a function of the Poisson's ratio for different materials and degrees of approximation.

(b) Different quality measures of the generated meshes with p=4 as a function of the Poisson's ratio for the ILE isotropic approach and using five load increments.

6 CONCLUSIONS

A consistently linearised solid mechanics based framework for the generation of high-order curvilinear meshes has been presented. The derivation of the approach, based on energy principles, is used to propose mesh quality measures based on independent invariants of the strain energy density. Of the three isotropic quality measures proposed, Q_3 is the most impactful indicator, which corresponds to the so-called scaled Jacobian traditionally used by the high-order mesh generation community.

In terms of the material parameters, the use of a Poisson's ratio near the incompressible limit is generally advised in order to maximise the quality of the resulting mesh. For isotropic meshes, a low number of increments (e.g. five increments) is typically sufficient to obtain the

maximum possible quality, whereas for highly stretched meshes and for high-orders of approximation (i.e. $p > 4$) a higher number (e.g. 40 increments) is needed to obtain good quality meshes.

ACKNOWLEDGMENTS

The first author acknowledges the financial support received through The Erasmus Mundus SEED program. The second author gratefully acknowledges the financial support provided by the Sér Cymru National Research Network in Advanced Engineering and Materials. The third author acknowledges the financial support received through The Leverhulme Prize awarded by The Leverhulme Trust, UK.

REFERENCES

[Dey, O'Bara, and Shephard] Dey S, O'Bara RM, Shephard MS (2001) Towards curvilinear meshing in 3D: the case of quadratic simplices. Computer-Aided Design 33(3):199 – 209

[Moxey, Ekelschot, Keskin, Sherwin, and Peiró] Moxey D, Ekelschot D, Keskin U, Sherwin S, Peiró J (2014) A thermo-elastic analogy for high-order curvilinear meshing with control of mesh validity and quality. Procedia Engineering 82(0):127 – 135, 23rd International Meshing Roundtable (IMR23)

[Persson and Peraire] Persson PO, Peraire J (2009) Curved mesh generation and mesh refinement using lagrangian solid mechanics. In: Proceedings of the 47th AIAA Aerospace Sciences Meeting and Exhibit, AIAA

[Poya, Sevilla, and Gil] Poya R, Sevilla R, Gil A (2016) A unified framework for a posteriori high-order curved mesh generation using solid mechanics. Under Review

[Vincent and Jameson(2011)] Vincent PE, Jameson A (2011) Facilitating the adoption of unstructured high-order methods amongst a wider community of fluid dynamicists. Math Model Nat Phenom 6(3):97–140

[Xie, Sevilla, Hassan, and Morgan] Xie ZQ, Sevilla R, Hassan O, Morgan K (2013) The generation of arbitrary order curved meshes for 3D finite element analysis. Computational Mechanics 51(3):361–374